Lateral carrier transfer in $Cd_xZn_{1-x}Se/ZnS_ySe_{1-y}$ quantum dot layers

S. Rodt,* V. Türck, R. Heitz, F. Guffarth, R. Engelhardt, U. W. Pohl, M. Straßburg, M. Dworzak, A. Hoffmann, and D. Bimberg

Institut für Festkörperphysik, Technische Universität Berlin, Hardenbergstraße 36, 10623 Berlin, Germany

(Received 14 November 2002; published 26 June 2003)

Lateral carrier transfer is investigated for single $Cd_xZn_{1-x}Se/ZnS_ySe_{1-y}$ quantum dots (QD's) in a high-density ensemble by time-resolved spectroscopy. Following nonresonant excitation a significant probability of independent capture of electrons and holes in separate QD's is observed. The subsequent lateral migration of carriers between adjacent QD's leads to a slow decay component of the exciton ground-state luminescence. At low temperatures the lateral carrier transfer is restricted to phonon-assisted inter-QD tunneling, resulting in migration times of the order of several nanoseconds. The role of independent carrier capture is suppressed at high excitation densities or increased temperatures, enabling thermally activated migration.

DOI: 10.1103/PhysRevB.67.235327 PACS number(s): 78.67.Hc, 72.20.Jv, 78.55.Et, 78.60.Hk

I. INTRODUCTION

Semiconductor quantum dots (QD's) grown epitaxially in the Stranski-Krastanow mode on planar substrates are presently the subject of intense studies.[1] The interest is largely driven by the simplicity of the fabrication of high-density ensembles of defect-free QD's and their application in optoelectronic devices, like lasers and detectors. A critical aspect in such applications is the lateral interaction of QD's, being essential for the carrier mobility within the QD layer and, thus, the steady-state carrier distribution. At sufficiently low temperatures and large inter-QD spacings the QD's act as independent recombination centers that are statistically populated.[2] The resulting carrier dynamics and, hence, statistics do not allow for an equilibrium description based on average occupation numbers and a global quasi-Fermi level. Either thermally activated escape followed by recapture or tunneling, which requires dense QD ensembles with sufficiently low tunnel barriers, might lead to inter-QD carrier transfer.[3–6] Efficient lateral carrier migration would result in the formation of a global Fermi-level and quantum-well like statistics.

As a consequence of the self-organized growth, the QD's are neither structurally identical nor homogeneously distributed, hampering the experimental investigation of the inter-QD interaction. The electronic coupling between neighboring QD's has been investigated for vertically stacked QD's,[7,8] for which the separating barrier can be controlled by modifying the spacer thickness and composition. Stacking of QD's, which intentionally differ in size or composition, was exploited for the investigation of energy transfer processes.[9,10] Theoretical investigations predicted electronic coupling for a spacer thickness below about 6 nm,[11] and fast nonresonant energy transfer was observed for asymmetric QD pairs with tunnel barrier widths below about 5 nm.[10] Note that the energy transfer is nonresonant even for nominally identical QD pairs due to the asymmetry of the built-in strain.[11]

The investigation of lateral carrier transfer processes within a dense QD layer is more difficult since neighboring QD's can neither be identified nor isolated. Here, the identification of lateral energy transfer is indirect, requiring to model the average effect on the ensemble properties. For QD ensembles with densities in excess of about 10^{11} cm^{-2}, a decrease of the decay time on the high-energy slope of the photoluminescence (PL) peak was observed and taken as evidence for lateral exciton transfer from smaller to larger QD's.[5,12–14] With increasing temperature, thermally activated escape to the wetting layer followed by recapture leads to an efficient redistribution of excitons among the QD's,[15] establishing ultimately a global quasi-Fermi level.[16] Obviously, the transfer of excitons between QD's can occur only during the exciton lifetime and, thus, affects the initial decay of the QD luminescence in the subnanosecond region.[12–14] Exciton transfer cannot account for *slower* decay components extending well beyond the exciton life span, which have been observed repeatedly for the ground-state luminescence of self-organized QD's.[17,18] For samples with a single layer of QD's such a slow component was tentatively attributed either to carrier feeding from tail states in the matrix[17] or to the coexistence of two different radiative exciton states, characterized by different spectral and temporal characteristics[18,19] For stacked pairs of asymmetric QD's such a slow component was attributed to the formation of spatially indirect excitons.[20] For colloidal CdSe QD's (Ref. 21) and alloy-disordered $Cd_xZn_{1-x}Se/ZnSe$ quantum wells[22] spin-flip from dark to bright exciton states might provide an intrinsic explanation for observed PL decay times, that are much longer than the radiative bright exciton lifetime.

A potential model system for studies of lateral carrier migration are $Cd_xZn_{1-x}Se$ layers in a ZnS_ySe_{1-y} matrix, which in suitable samples form a high-density ($>10^{11}$ cm^{-2}) ensemble of weakly localizing QD's. Such properties favor inter-QD tunneling and, thus, lateral carrier migration within the QD layer. Time-resolved experiments show in addition to the well-known direct exciton decay a slow decay component with time constants of some nanoseconds for the ground-state luminescence, which is demonstrated to result from the bright exciton decay. The results of time-resolved cathodoluminescence (TRCL) investigations of single QD's and time-resolved photoluminescence (TRPL) experiments of the ensemble indicate lateral migration of carriers in the $Cd_xZn_{1-x}Se/ZnS_ySe_{1-y}$ QD layer due to inter-QD tunneling.

II. EXPERIMENTAL

The investigated samples were grown by low-pressure metalorganic chemical vapor phase epitaxy, as described in Ref. 23. About 1.7 monolayer CdSe were embedded in a $ZnS_{0.06}Se_{0.94}$ matrix at a temperature of 350 °C. Previous structural and optical investigations indicated a rather complex potential landscape: Pronounced Zn and Cd interdiffusion leads to a two-dimensional (2D)-like $Cd_xZn_{1-x}Se$ layer with lateral variations of the Cd concentration on a few-nm length scale-creating a high density ($>10^{11}$ cm^{-2}) of QD's within this layer.[23]

PL and PL excitation (PLE) measurements were done with a tungsten lamp dispersed by a 0.27-m double-grating monochromator as tunable excitation source and a bi-alkali photomultiplier in combination with a 0.3-m double-grating monochromator for detection. Spatially resolved cathodoluminescence (CL) measurements were performed in a JEOL JSM 840 scanning electron microscope with the sample mounted on the cold finger of a temperature-variable He-flux cryostat and an acceleration voltage of 7 kV. The luminescence light was dispersed by a 0.3-m spectrometer equipped with a 2400-grooves/mm grating and detected with a N_2-cooled back-illuminated Si-CCD, providing for a spectral resolution of 290 μeV. To study reproducibly individual QD's in CL platinum shadow masks were fabricated on the samples.[24] For TRCL experiments the exciting electron beam was pulsed by a capacitive beam blanking unit and transients were recorded by time-correlated single-photon counting with a multichannel-plate photomultiplier. The square shaped excitation pulse with a length of 7 ns ensured quasi-cw starting conditions and the steep switch-off slope did provide for a time resolution better than 50 ps. TRPL experiments used 4 ps pulses of a cavity-dumped, synchronously pumped dye laser. The repetition rate of 3.8 MHz provided for a sufficient wide time window to monitor the slow component. The luminescence was spectrally dispersed by a subtractive 0.35 m double-grating monochromator. The system response had a full width at half maximum (FWHM) of 20 ps.

III. EXPERIMENTAL RESULTS AND DISCUSSION

A typical luminescence spectrum of the investigated $Cd_xZn_{1-x}Se/ZnS_ySe_{1-y}$ QD sample is shown in Fig. 1(a). In addition to the ZnS_ySe_{1-y} matrix luminescence at 2.835 eV the emission of the QD ensemble appears at 2.615 eV with a FWHM of 60 meV.

PLE measurements provide information on the electronic properties of the QD's in the ensemble, in particular, on the exciton localization and the 2D inter-QD coupling in the $Cd_xZn_{1-x}Se$ layer. The latter leads to a mobility edge in the $Cd_xZn_{1-x}Se$ layer, which might be identified as the wetting layer.[12] Figure 1(b) shows a contour plot of the PL intensity as a function of the detection and excitation energies with the luminescence intensity given on a logarithmic scale. The contour plot was generated from a series of PLE spectra stepping the detection energy across the inhomogeneously broadened PL peak [gray shaded area in Fig. 1(a)]. Horizontal (vertical) cuts correspond to PL (PLE) spectra for the

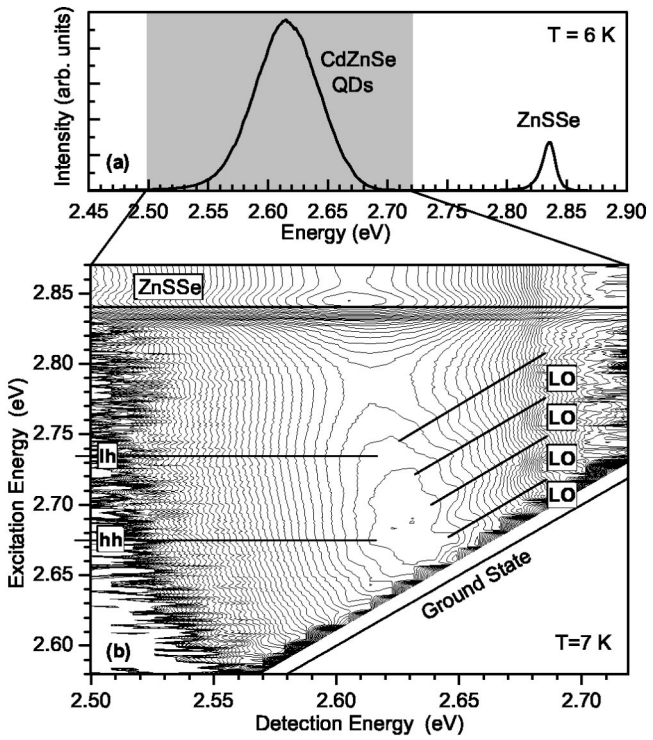

FIG. 1. (a): Temporally and spatially integrated CL spectrum. (b) PLE contour plot. The range of detection energies is marked by the gray area in (a) and the intensity is given on a logarithmic scale. Black lines denote on the low-energy side light-hole (lh) and heavy-hole (hh) resonances of the 2D-like $Cd_xZn_{1-x}Se$ layer and on the high-energy side LO-phonon resonances due to hot-exciton relaxation.

respective excitation (detection) energy. The band edge of the ZnS_ySe_{1-y} matrix shows up as a horizontal step at an excitation energy of 2.84 eV. The broad steps in the PLE efficiency at about 2.675 eV and 2.735 eV, which are observed probing the low-energy tail of the QD emission, are attributed to the average energies of the heavy-hole (hh) and light-hole (lh) transitions of the 2D-like $Cd_xZn_{1-x}Se$ layer, respectively. The large FWHM of the excitation resonances suggests a considerable spatial variation of the corresponding transition energies. Indeed, the observation of QD luminescence with energies higher than the average hh-transition energy suggests the existence of localized states in higher-energy regions of the $Cd_xZn_{1-x}Se$ layer. For those QD's with high-energy emissions the optical results support the capture into the QD's to compete with lateral migration. On the one hand, the PLE spectra show pronounced LO-phonon resonances probing the high-energy tail of the QD PL. Only QD's, that can be reached directly by LO-phonon scattering are populated efficiently, otherwise lateral migration to lower-energy regions of the 2D-layer dominates. The period of $\sim$31 meV is close to the LO-phonon energy of ZnSe.[25] Similar phonon features have previously been taken as indication for hot exciton relaxation in III-V based QD samples.[26] On the other hand, the PL peak shows a blueshift of about 30 meV going from nonresonant to near-resonant excitation. The population of the high-energy QD's is efficient only for near-resonant excitation.

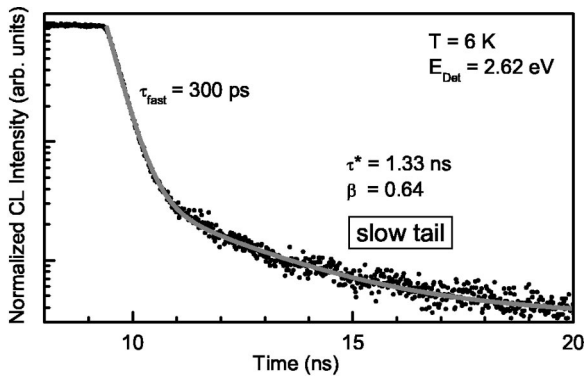

FIG. 2. Transient of the QD ensemble showing in addition to the initial exciton recombination a slow tail. The transient was taken at 2.62 eV on the maximum of the QD ensemble luminescence. The solid line is a fit with a stretched exponential function, as described in the text.

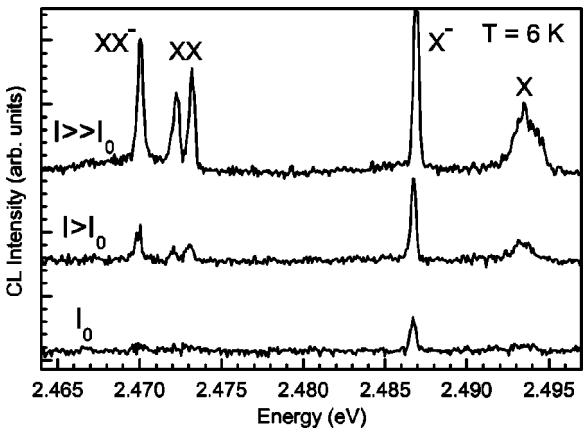

FIG. 3. Time-integrated CL spectra of a single QD for different excitation densities. The excitation densities are given relative to the lowest one (I_0). The spectra are shifted vertically for clarity.

The PLE measurements [Fig. 1(b)] show that the $Cd_xZn_{1-x}Se$ layer presents a complex potential landscape providing localization sites with a broad spectrum of localization energies, which are generally well below 150 meV. Considering the high density of QD's ($>10^{11}$ cm^{-2}) and the low potential barriers between the QD's lateral energy transfer processes are expected to be important.

A typical luminescence transient of an ensemble of QD's with a ground-state transition energy of 2.62 eV is shown in Fig. 2. The transient was measured by TRCL integrating over a 6×5 μm^2 sample area. The transients show typically two clearly distinguished components: A fast initial exponential decay and a slow non-exponential tail. The initial exponential decay with a typical time constant $\tau_{\text{fast}}=300$ ps is attributed to the recombination of excitons formed by the direct capture of excitons or of electron-hole pairs into the QDs. The time constant is typical for the radiative recombination of excitons in such II-VI QD's.[27] Detailed TRPL investigations of this fast decay show a pronounced decrease of the decay time on the high-energy slope of the QD luminescence peak, which can be attributed to lateral exciton transfer processes between QD's.[12] Here, we concentrate on the slow non-exponential tail, extending over tens of nanoseconds, which will be shown to result from the lateral migration of carriers in the $Cd_xZn_{1-x}Se$ layer. The tail cannot be described by a single exponential function but by a so-called stretched exponential one:[28]

$$I(t)=I_0\exp[-(t/\tau^{\star})^{\beta}]. \tag{1}$$

Equation (1) describes a nonseparable superposition of different exponential decay processes, with $\tau^{\star}$ being an effective time constant and β the so-called stretching parameter. The latter describes the spread of the time constants and is 1 for a mono-exponential decay. Probing an ensemble of QD's as in Fig. 2 the slow component is fitted well by Eq. (1), yielding effective time constants of about 1.3 ns and stretching parameters β around 0.6. A stretching parameter well below one indicates a significant variation of the exponential time constants in the slow tail. Considering that an ensemble of QD's is probed the variation might be attributed to varying properties of the single QD's. Further insight into the origin of the slow component requires then the investigation of single QD's. Figure 3 shows the emission of a single $Cd_xZn_{1-x}Se/ZnS_ySe_{1-y}$ QD measured through a 80-nm wide aperture at different excitation densities. As shown before,[29] the labeled line groups originate from the recombination of neutral and negatively charged excitons (X) and biexcitons (XX). Lowering the excitation density only exciton recombination remains, whereby recombination of negatively charged excitons (marked X^-) dominates. The preferential formation of charged excitons is attributed to an unintentional *n*-type background in the investigated samples. Time-resolved single-QD experiments were performed with an excitation density corresponding to the topmost spectrum in Fig. 3, exciting both excitons and biexcitons.

Information on the spatial distribution of the slow and fast component are provided by monochromatic time-delayed images of the luminescence intensity across the sample surface, as depicted in Fig. 4. The detection energy was 2.469 eV and panels (a), (b), and (c) correspond, respectively, to the in-pulse equilibrium, to the fast recombination of exciton complexes, and to the slow component [the time windows are indicated in Fig. 4(d)]. The bright spots in panel (a) correspond to QD's for which the recombination of one of the possible exciton complexes (Fig. 3) is resonant to the detection energy.[30] As evident from panel (b) all these recombination processes exhibit a fast decay. Panel (c) demonstrates that the slow component originates from the same QD's, although it is observed only for some of them (marked by arrows).

The time-delayed images suggest that the slow component is observed only for certain exciton complexes. This is confirmed by time-delayed spectra measured for an about 100 nm wide aperture, Fig. 5(b). The slow decay component is observed only for some of the emission lines: Two of the four emission lines exhibit the fast decay only, while the other two lines show also the slow tail. Panels (a) and (c) show time-delayed spectra corresponding to the fast and slow decay components, respectively. The time-resolved experiments on single QD's demonstrate unambiguously that

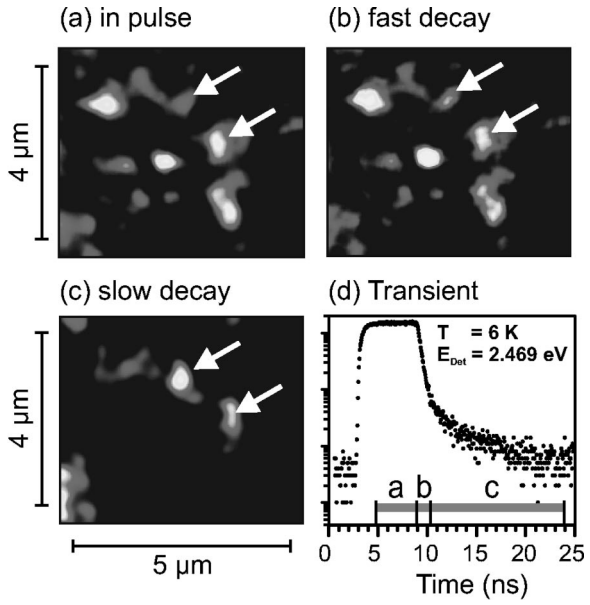

FIG. 4. Time-delayed monochromatic CL pictures of a 5 μm $\times$4 μm sample area. The pictures show the time-integrated luminescence during the excitation pulse (a), during the fast decay (b), and during the slow decay (c). Panel (d) depicts an ensemble transient detected at 2.469 eV and shows the respective time windows of the pictures. The arrows mark two QD's that show the slow decay component.

both the fast and slow component originate from the very same transition, i.e., the recombination of the same exciton state. The only possible explanation are two different excitation channels. On the one hand, the direct capture of nonresonantly excited excitons or electron-hole pairs is too fast to be resolved in the present experiments. The subsequent decay of the localized exciton is the fast initial decay in the transients, whereby the decay time corresponds to the radiative exciton lifetime. The slow component, on the other hand, indicates obviously a slow feeding process from an intermediate metastable state. The decay time corresponds to the lifetime of the intermediate state.

The present results are strikingly different from those recently reported for CdSe/ZnSe QD's, for which a similar slow tail was observed in the transients.[18] It was proposed that the single sharp emission lines observed in spatially resolved PL originate from a metastable QD state, whereas the fast initial decay ($\sim$450 ps) is associated with a QD state that leads to broad luminescence structures of up to several 10 meV halfwidths. This analysis of the experimental results is in conflict to the general accepted interpretation of the fast decay time as the radiative lifetime of the localized excitons.[27] The TRCL results for single QD's presented here suggest that the higher density of emission lines during the initial fast decay might have prevented the identification of single emission lines, whereas single lines could be resolved after a delay of some nanoseconds when the number of emission lines is significantly reduced. For the $Cd_xZn_{1-x}Se/ZnS_ySe_{1-y}$ QD structures investigated here both the fast and slow decay component can be unambiguously attributed to the very same electronic transition,

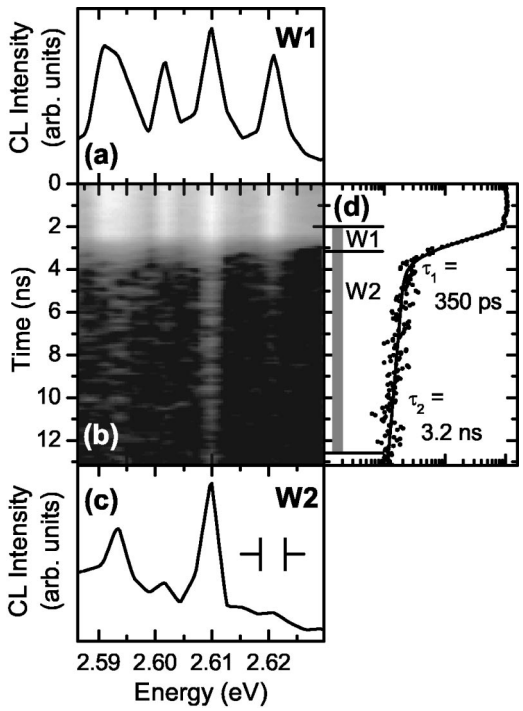

FIG. 5. Time-delayed CL spectra showing the temporal evolution of four single QD emission lines (b). (d) shows the transient extracted at 2.61 eV. Dots are measured values, the solid line is a biexponential fit of the transient. Spectra (a) and (c) are taken in the time windows *W*1 and *W*2, respectively, demonstrating that the fast and the slow decay occur at the same emission energy. The sample temperature was 6 K.

providing experimental access to inter-QD carrier tunneling.

Figure 6 compares transients with a slow tail for different QD's. Each of the single-QD transients is fitted well by a biexponential decay with the decay time of the slow component varying between 2.01 ns and 4.64 ns. Fits by Eq. (1) yield within the experimental uncertainty stretching parameters of 1. The mono-exponential character of the slow tail is consistent with a well-defined energy transfer process, e.g.,

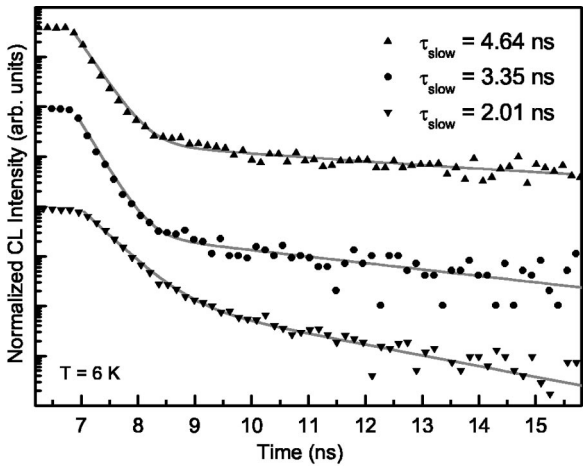

FIG. 6. CL transients of different QD's. Solid lines are biexponential fits of the transients. The transients are shifted vertically for clarity.

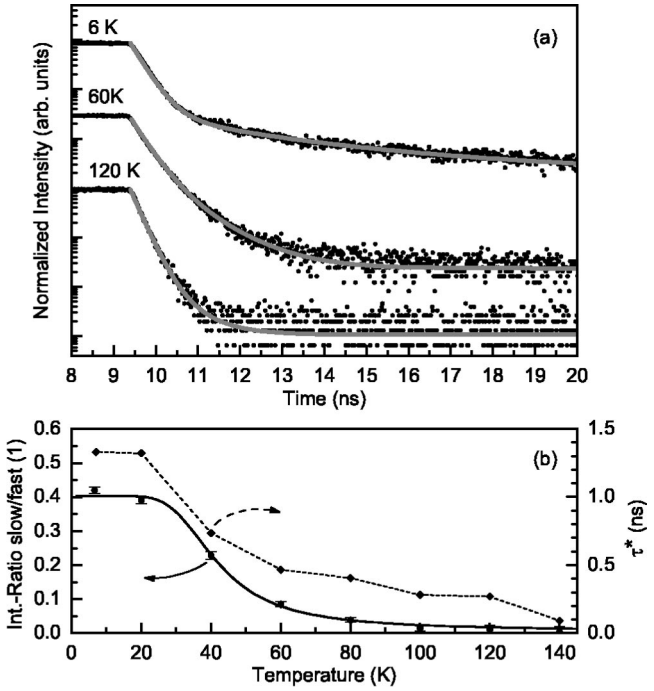

FIG. 7. (a) Transients of the QD luminescence measured by spatially integrated TRCL at three temperatures. The transients were taken on the maximum of the QD ensemble luminescence and are shifted vertically for clarity. Solid lines are fits with stretched exponential functions. (b) Left axis: intensity ratio of the slow and the fast components as a function of temperature. The solid line is a fit assuming thermally activated carrier migration, yielding an activation energy of 17 meV; right axis: temperature dependence of the effective time constant of the slow component.

between neighboring QD's. The decay time being at least one order of magnitude slower than typical exciton lifetimes indicates the transfer of single carriers, which finally combine to an exciton in a single QD. Obviously, such a slow carrier-feeding process can only support linear emission processes such as the recombination of neutral and charged excitons. Note that the Coulomb blockade reduces the probability of doubly charged QD's, which would be a precondition for the observation of a charged exciton during the slow tail. Thus, neutral exciton recombination is expected to dominate the slow tail.

In order to estimate the localization energy of the feeding centers the temperature dependence of the luminescence dynamics was investigated by TRCL for the QD ensemble, Fig. 7. Panel (a) shows spatially integrated transients for 6 K, 60 K, and 120 K, respectively, each being fitted well by a stretched exponential. Panel (b) shows the temperature dependence of the intensity ratio of the slow and the fast component (dots) as well as of the effective time constant $\tau^{\star}$ of the slow decay component (diamonds). Increasing the temperature above about 20 K the slow component becomes faster and starts to loose intensity with respect to the fast component, which is consistent with thermally activated emission of carriers from the feeding centers bypassing the temperature-independent tunneling. Fitting the intensity ratio with an Arrhenius-type function yields an activation energy

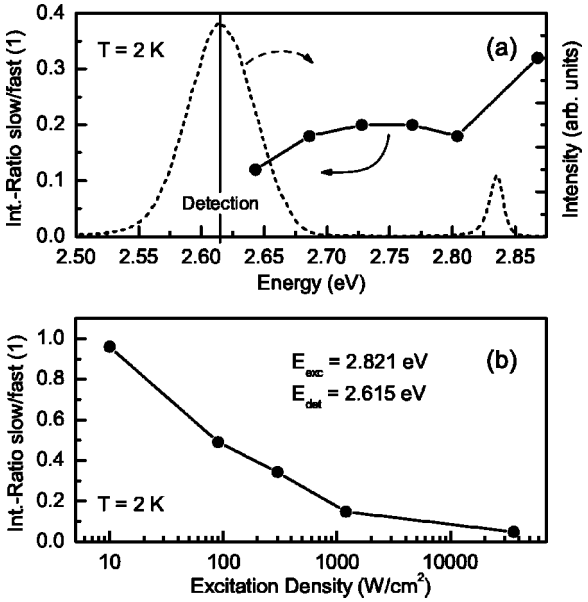

FIG. 8. Intensity ratio of the slow and the fast component for (a) different excitation energies and for (b) different excitation densities as measured by TRPL. The dashed line in panel (a) shows the PL spectrum. The detection energy for the time-resolved measurements in (a) was 2.615 eV.

of about 17 meV. The activation energy is some measure for the height of the tunneling barrier.

Information on the location of the feeding centers within the sample structure is obtained from time-resolved photoluminescence experiments, which allow to tune the excitation energy from above barrier excitation to resonant excitation of the $Cd_xZn_{1-x}Se$ layer. Figure 8(a) shows the corresponding evolution of the intensity ratio of the slow and the fast decay components. Apparently, the slow component can be excited resonantly via the $Cd_xZn_{1-x}Se$ layer, indicating the feeding centers to be directly connected with this layer. We suggest that the slow component results from the separate capture of electrons and holes in different $Cd_xZn_{1-x}Se$ QD's, followed by nonresonant lateral carrier transfer, which eventually leads to the observed localized excitons. Note that the activation energy of 17 meV is consistent with the smaller QD's in the ensemble to act as feeding centers. The increase of the relative intensity of the slow component exciting the ZnS_ySe_{1-y} barrier might result from additional feeding centers in the ZnS_ySe_{1-y} barrier. With increasing excitation density, the slow component vanishes, as shown in Fig. 8(b). An increasing occupation of the QD's reduces the number of charged QD's and, thus, the impact of lateral carrier transfer.

Our experimental results are unambiguously explained by lateral energy transfer processes within the $Cd_xZn_{1-x}Se$ layer, whereby the long time constants result from tunneling of single carriers between charged QD's, leading eventually to the formation of radiative, spatially direct excitons. At low temperatures, lateral carrier transfer will require phonon-assisted tunneling between, in general, the nonresonant localized states of neighboring QD's. The tunneling rate depends exponentially on the height and width of the lateral barrier between such QD pairs as well as on the energy mismatch.

Schroeter *et al.*[31] investigated theoretically energy transfer between QD and defect states, predicting the required tunneling rates in the nanosecond region for barrier thicknesses of only a few nanometers. Such barrier widths are in good agreement with the large density of the QD's in the $Cd_xZn_{1-x}Se$ layer ($>10^{11}$ cm^{-2}) and the small barrier height further accelerates tunneling. In Ref. 17 a similar slow decay component was reported for $InP/Ga_xIn_{1-x}P$ QD's, which, however, occurs only exciting nonresonantly in the $Ga_xIn_{1-x}P$ matrix. Obviously, lateral carrier transfer between neighboring QD's in the InP layer is negligible: The comparable large average separation of the QD's in the low-density ($\sim 10^{10}$ cm^{-2}) ensemble and the higher tunnel barriers suppress inter-QD tunneling.

Lateral carrier transfer also explains the non-exponential character of the slow component probing an ensemble of QD's. The statistically varying inter-QD separation, i.e., the thickness of the tunneling barrier, will be reflected in the tunneling rate. Thus, for each individual QD-pair an exponential slow component is expected, though the time-constant will vary with the probed QD. This behavior is indeed observed probing single QD's, as shown in Fig. 6. Above about 20 K thermal escape and recapture of charge carriers in the QD ensemble becomes faster than phonon-assisted tunneling, accelerating the slow component.

Finally, we note that slow feeding of the bright exciton state can occur intrinsically by spin-flip processes when initially the dark exciton state is populated. Indeed, the population of the dark exciton state plays a significant role for the exciton dynamics in colloidal CdSe QDs, accounting for low-temperature lifetimes of up to 1 μs.[21] The slow component of the bright exciton recombination in the self-organized $Cd_xZn_{1-x}Se/ZnS_ySe_{1-y}$ QDs studied here, however, cannot be attributed to the dark exciton state, which lies about 3 meV below the bright one.[32] In order to be consistent with a bright exciton lifetime of 300 ps and a spin-flip time of less than 10 ns at $T=10$ K the dark-bright exciton splitting would have to be smaller than 150 μeV. However, both experimental and theoretical investigations of epitaxial II-VI QD's suggest an at least one order of magnitude larger splitting. Indeed, recent reports support strongly suppressed spin-flip processes in self-organized QD's.[33] Furthermore, spin-flip processes from the dark-exciton state would result in an exponential increase of the decay time of the slow component with decreasing temperature. In contrast, we find the decay time to be almost constant below ≈ 20 K (Fig. 7), which is inconsistent with spin-flip processes but expected for lateral carrier tunneling within the $Cd_xZn_{1-x}Se$ layer.

IV. CONCLUSION

The carrier dynamics in a high-density ensemble of $Cd_xZn_{1-x}Se/ZnS_ySe_{1-y}$ QD's has been investigated by PLE and time-resolved PL and CL measurements. Luminescence transients observed both for the QD ensemble and for single QD's exhibit two decay components: A fast one with a typical time constant of 300 ps that is attributed to the radiative decay of exciton complexes formed instantly in the QD's and a slow one of the order of some nanoseconds. The slow component is demonstrated to result from a slow feeding of the exciton groundstate, which is attributed to lateral carrier migration within the $Cd_xZn_{1-x}Se$ QD layer eventually forming the observed exciton in single QD's. At He-temperature nonresonant tunneling is the main migration process, whereas at higher temperatures thermally activated transfer dominates.

ACKNOWLEDGMENTS

We thank R. Steingrüber from Heinrich-Hertz-Institute for professional e-beam lithography. Part of this work was funded in the framework of Sonderforschungsbereich 296 of Deutsche Forschungsgemeinschaft.

*Electronic address: srodt@physik.TU-Berlin.DE

[1] D. Bimberg, M. Grundmann, and N.N. Ledentsov, *Quantum Dot Heterostructures* (Wiley, Chichester, 1999).
[2] M. Grundmann and D. Bimberg, Phys. Rev. B **55**, 9740 (1997).
[3] D.L. Huffaker and D.G. Deppe, Appl. Phys. Lett. **73**, 366 (1998).
[4] D.L. Huffaker, L.A. Graham, and D.G. Deppe, Appl. Phys. Lett. **72**, 214 (1998).
[5] A. Tackeuchi, Y. Nakata, S. Muto, Y. Sugiyama, T. Usuki, Y. Nishikawa, N. Yokoyama, and O. Wada, Jpn. J. Appl. Phys., Part 2 **34**, L1439 (1995).
[6] D.G. Deppe and Q. Deng, Appl. Phys. Lett. **73**, 3536 (1998).
[7] N.N. Ledentsov, V.A. Shchukin, M. Grundmann, N. Kirstaedter, J. Böhrer, O. Schmidt, D. Bimberg, V.M. Ustinov, A.Yu. Egorov, A.E. Zhukov, P.S. Kop'ev, S.V. Zaitsev, N.Yu. Gordeev, Zh.I. Alferov, A.I. Borovkov, A.O. Kosogov, S.S. Ruvimov, P. Werner, U. Gösele, and J. Heydenreich, Phys. Rev. B **54**, 8743 (1996).
[8] G.S. Solomon, J.A. Trezza, A.F. Marshall, and J.S. Harris, Jr., Phys. Rev. Lett. **76**, 952 (1996).
[9] A. Tackeuchi, T. Kuroda, K. Mase, Y. Nakata, and N. Yokoyama, Phys. Rev. B **62**, 1568 (2000).
[10] R. Heitz, I. Mukhametzhanov, P. Chen, and A. Madhukar, Phys. Rev. B **58**, R10151 (1998).
[11] A. Schliwa, O. Stier, R. Heitz, M. Grundmann, and D. Bimberg, Phys. Status Solidi B **224**, 405 (2001).
[12] M. Straßburg, M. Dworzak, H. Born, R. Heitz, A. Hoffmann, M. Bartels, K. Lischka, D. Schikora, and J. Christen, Appl. Phys. Lett. **80**, 473 (2002).
[13] F. Gindele, U. Woggon, W. Langbein, J.M. Hvam, K. Leonardi, D. Hommel, and H. Selke, Phys. Rev. B **60**, 8773 (1999).
[14] S. Yamaguchi, Y. Kawakami, S. Fujita, S. Fujita, Y. Yamada, T. Mishina, and Y. Masumoto, Phys. Rev. B **54**, 2629 (1996).
[15] W. Yang, R.R. Lowe-Webb, H. Lee, and P.C. Sercel, Phys. Rev. B **56**, 13 314 (1997).
[16] M. Grundmann, Physica E (Amsterdam) **5**, 167 (2000).
[17] T. Okuno, H.-W. Ren, M. Sugisaki, K. Nishi, S. Sugou, and Y. Masumoto, Phys. Rev. B **57**, 1386 (1998).
[18] L.M. Robinson, H. Rho, J.C. Kim, H.E. Jackson, L.M. Smith, S. Lee, M. Dobrowolska, and J.K. Furdyna, Phys. Rev. Lett. **83**, 2797 (1999).
[19] S. Lee, J.C. Kim, H. Rho, C.S. Kim, L.M. Smith, H.E. Jackson, J.K. Furdyna, and M. Dobrowolska, Phys. Rev. B **61**, R2405 (2000).
[20] R. Heitz, I. Mukhametzhanov, O. Stier, A. Hoffmann, A.

Madhukar, and D. Bimberg, *Physics and Applications of Semiconductor Quantum Structures*, edited by J.-C. Woo and T. Yao (IOP Publishing, Bristol, 2001).

[21] M. Nirmal, D.J. Norris, M. Kuno, M.G. Bawendi, Al.L. Efros, and M. Rosen, Phys. Rev. Lett. **75**, 3728 (1995).

[22] J. Puls, F. Henneberger, M. Rabe, and A. Siarkos, J. Cryst. Growth **184/185**, 787 (1998).

[23] R. Engelhardt, U.W. Pohl, D. Bimberg, D. Litvinov, A. Rosenauer, and D. Gerthsen, J. Appl. Phys. **86**, 5578 (1999).

[24] V. Türck, S. Rodt, O. Stier, R. Heitz, R. Engelhardt, U.W. Pohl, D. Bimberg, and R. Steingrüber, Phys. Rev. B **61**, 9944 (2000).

[25] H. Tews, G. Neu, and J. De-Sheng, Phys. Rev. B **24**, 7321 (1981).

[26] R. Heitz, M. Veit, N.N. Ledentsov, A. Hoffmann, D. Bimberg, V.M. Ustinov, P.S. Kop'ev, and Zh.I. Alferov, Phys. Rev. B **56**, 10 435 (1997).

[27] G. Bacher, R. Weigand, J. Seufert, V.D. Kulakovskii, N.A. Gippius, A. Forchel, K. Leonardi, and D. Hommel, Phys. Rev. Lett. **83**, 4417 (1999).

[28] X. Chen, B. Henderson, and K.P. O'Donnell, Appl. Phys. Lett. **60**, 2672 (1992).

[29] V. Türck, S. Rodt, R. Heitz, O. Stier, M. Straßburg, U.W. Pohl, and D. Bimberg, Phys. Status Solidi B **224**, 217 (2001).

[30] The apparent size of the QD's is determined by the effective excitation volume with a diameter of about 400–500 nm for the chosen acceleration voltage of 7 kV.

[31] D.F. Schroeter, D.J. Griffiths, and P.C. Sercel, Phys. Rev. B **54**, 1486 (1996).

[32] V.D. Kulakovskii, G. Bacher, R. Weigand, T. Kümmell, A. Forchel, E. Borovitskaya, K. Leonardi, and D. Hommel, Phys. Rev. Lett. **82**, 1780 (1999).

[33] V.K. Kalevich, M. Paillard, K.V. Kavokin, X. Marie, A.R. Kovsh, T. Amand, A.E. Zhukov, Yu.G. Musikhin, V.M. Ustinov, E. Vanelle, and B.P. Zakharchenya, Phys. Rev. B **64**, 045309 (2001).